Superexchange Interactions through Quasi-Linear End-to-End Azido Bridges: Structural and Magnetic Characterisation of a New Two-Dimensional Manganese–Azido System $[Mn(DENA)_2(N_3)_2]_n$ (DENA = diethylnicotinamide)

Mohamed A. S. Goher,[a] Morsy A. M. Abu-Youssef,[a] Franz A. Mautner,[b] Ramon Vicente,[c] and Albert Escuer*[c]

Keywords: Manganese / Two-dimensional systems / Azido bridges

Reaction of sodium azide with manganese(II) and diethylnicotinamide (DENA) leads to the two-dimensional system *trans*-$[Mn(DENA)_2(N_3)_2]_n$. The compound crystallises in the *P*2/*c* (monoclinic) group. Structural determination shows layers of manganese atoms bridged by means of single $\mu_{1,3}$-azido bridges. The polymeric structure is achieved by means of two different $\mu_{1,3}$-azide bridges, one of them with Mn–N–N bond angles of 148.4(2)°, whereas the second nonequivalent azido bridge has the unusual feature of quasi-linear coordination with Mn–N–N bond angles of 171.7(2)°. Molecular orbital calculations and susceptibility data show antiferromagnetic interaction and similar constant coupling values for the two superexchange pathways, in spite of the structural differences. Susceptibility, magnetisation, and EPR properties are compared with related azido systems.

Introduction

Manganese-azide compounds in which the azide ligand acts as a bridge exclusively in the end-to-end coordination mode (EE) have recently been developed. The number of reported compounds is limited to seven, but there is an exceptional versatility of topologies and magnetic properties: one dinuclear system has a single quasi-linear EE bridge,[1] there are three chains with double EE azido bridges,[2,3] two 2-D systems[4,5] and one 3-D compound,[6] in which each of the manganese atoms is coordinated to the four neighbouring manganese atoms by means of four single EE bridges, and, finally, one 3-D system with each manganese atom octahedrally surrounded by six EE bridges. 1[7]

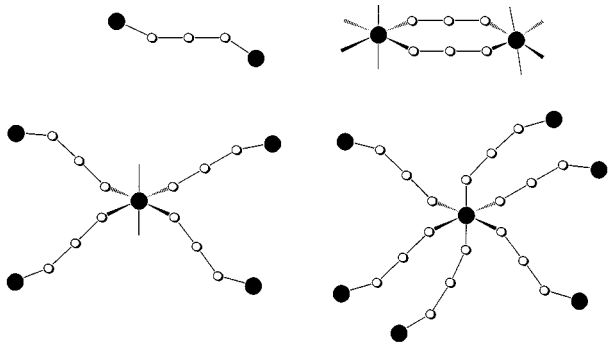

Scheme 1. Basic units found to date for Mn^{II}/end-to-end azide systems

[a] Chemistry Department, Faculty of Science, Alexandria University, P.O.Box. 426, Ibrahimia, Alexandria 21321, Egypt
[b] Institut für Physikalische und Theoretische Chemie, Technische Universität Graz, A-8010 Graz, Austria
[c] Departament de Química Inorgànica, Universitat de Barcelona, Diagonal 647, 08028 Barcelona, Spain
E-mail: aescuer@kripto.qui.ub.es

Magnetically, all of them show antiferromagnetic interactions, even the quasi-linear EE bridge. The magnetic properties for the two general cases of single[6b] or double[2] EE bridge correlate with the bond structural parameters (mainly bond angles) that determine the overlap of the MO of the bridge with the adequate AO of the manganese atoms. Interest in this kind of compound was reinforced by the characterisation of long-range magnetic ordering with spontaneous magnetisation below T_C = 28 K for the 2-D $[Mn(4\text{-acpy})_2(N_3)_2]_n$ system, (4-acpy = 4-acetylpyridine).[8a]

The EE bridge has also been found in other kinds of 1-D, 2-D honeycombs, or 3-D alternating systems together with a second kind of bridge, such as the end-on azido bridge (EO)[2,6b,8] or other ligands such as 4,4'-bipyridine[9] or bipyrimidine.[10] However, in these cases, the intrinsic difficulties in determining the *J* values makes it difficult to correlate the magnitude of the coupling with structural data.[10c]

Following our research on compounds of this kind, we studied the derivative obtained from the reaction of manganese(II) with diethylnicotinamide (DENA) and sodium azide. The new two-dimensional system *trans*-$[Mn(DENA)_2(N_3)_2]_n$ was structurally characterised; this compound consists of well-isolated layers in which the manganese atoms are bridged by four azido ligands (two pairs of nonequivalent bridges) in the EE mode, showing the expected antiferromagnetic coupling. One of these nonequivalent EE bridges shows quasi-linear Mn–N–N–N–Mn coordination, with Mn–N–N bond angles of 171.7°, far from the preferred bond angles derived from the sp^2 arrangement of the terminal nitrogen atoms of the ligand. It should be emphasised that constrained linear $\mu_{1,3}$-coordination for azido bridges has been found only recently through the use of systems in which the two paramagnetic ions are placed in rigid cryptand ligands.[1]

  1434–1948/00/0808–1819 $ 17.50+.50/0

In this paper we present the synthesis, structural characterisation, magnetic behaviour (focusing our attention on the exceptional linear azido bridge), and EPR data for $[Mn(DENA)_2(N_3)_2]_n$, together with a comparison with the previously reported end-to-end manganese–azido systems.

Results and Discussion

Crystal Structure of $[Mn(DENA)_2(N_3)_2]_n$ (1)

The structure of **1** consists of 2D manganese–azido sheets. A labelled ORTEP plot of the asymmetric unit is shown in Figure 1 Manganese atoms are placed in a centrosymmetric octahed al environment. The coordination polyhedron is formed by two DENA and four azido ligands coordinated in a *trans* arrangement, elongated along the axis defined by the pyridinic ligands, Mn–N(1) = 2.291(3) and similar Mn–N azido distances Mn–N(11) = 2.210(3) and Mn–N(21) = 2.225(3) Å. Each azido ligand acts as a bridge to the next manganese atom in the end-to-end coordination mode, allowing a two-dimensional polymer in the *bc* plane (Figure 2). Whereas the bond angle Mn–N(21)–N(22) = 148.4(2)° lies in the normal range for this kind of compound,[2,7] Mn–N(11)–N(12) = 171.7(2)° shows a quasi-linear coordination which has to date only been reported for systems with strong sterical constraints, such as cryptand compounds. The Mn–azido–Mn torsion angle, defined as the Mn–N(11)–N(12)–N(11C)–Mn(1C) dihedral angle, is 180°, whereas Mn–N(21)–N(22)–N(21A)–Mn(1A) has a torsion angle value of 166.7(2)°. Due to these asymmetric bond angles and the Mn–N_3–Mn torsion angle, the planes defined by the neighbouring manganese atom and the four bonded N (azido) atoms show a low dihedral angle of 5.6°. Minimum Mn–Mn intraplane distances are 6.553(3) Å and 6.695(3) Å, whereas the shorter interplane distance is 14.153 Å (*x* axis of the cell) due to the large space occupied by the pyridine ligands which isolate the manganese–azide layers (Figure 2). The general trends of the structure of **1** is similar to that of the two-dimensional compounds with 4-acetylpyridine or methylisinicotinate ligands;[4,5] the most significant differences are the more asymmetric Mn–N–N and Mn–N···N–Mn bond angles (Table 1).

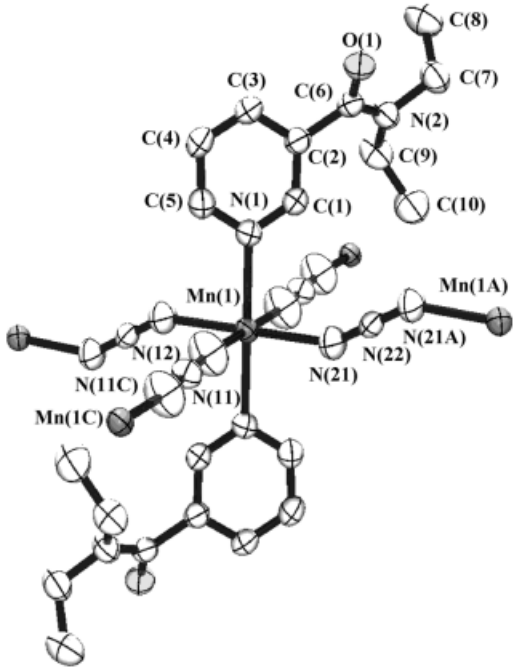

Figure 1. ORTEP drawing of $[Mn(DENA)_2(N_3)_2]_n$; ellipsoids at 50% probability level

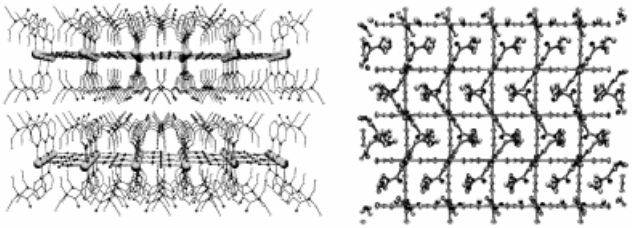

Figure 2. View of the $[Mn(DENA)_2(N_3)_2]_n$ compound along the (0 0 1) direction, to show the large interplane separation induced by the large pyridinic ligand (left); view along the (1 0 0) direction, showing the quadratic manganese–azide network

Table 1. Comparative structural and magnetic data for the three two-dimensional manganese–EE azide systems structurally characterised to date. "Angl. mean planes" refers to the angle between the MnN_4 (*N*-azide) planes; intersheet *d* is the minimum Mn–Mn interplane distance; ΔHpp is the EPR linewidth at room temperature; T_C indicates the ordering temperature, if present.

	L = DENA	L = 4-acpy	L = Me-*i*-nic
Mn–N–N	148.4°/171.7°	129.0°/151.6°	128.3°/149.7°
Mn–N···N–Mn	180°/166.7°	100.4°	96.8°
Angle's mean planes	5.65°	83.3°	84.9°
Intersheet *d* [Å]	14.153	11.563	12.424
J [cm^{-1}]	–3.42	–3.83	–2.24
ΔHpp [*G*]	30	30	46
T_C	$T_C < 2$	28 K	$T_C < 2$
ref.	this study	[4, 8a]	[5]

Superexchange Mechanism

Structural date enable two different superexchange pathways to be proposed, one through the azido bridge, with Mn–N–N bond angles of 148.4° (J_1), and a second through the azido bridge, with Mn–N–N bond angles of 171.7° (J_2). Previous MO calculations[6b] on the single azido bridge for manganese(II) systems (d^5 configuration) show that when the bond angle increases and approaches 180°, the interaction through the dz^2 orbitals of the paramagnetic centres and the nonbonding π orbitals of the bridge decreases, tending to zero for the 180° bond angle, whereas the overlap between the d*xz* and d*yz* atomic orbitals and the π orbitals of the bridge increases to the maximum interaction at 180°. In our case, we performed the MO calculations for the experimental bond angles, according to the molecular simulation previously proposed, and using as input parameters the experimental Mn–N(azide), N–N bond lengths and the experimental Mn–N–N and M–N–N–N–Mn bond and tor-

sion angles. The results of the calculations,[11] plotted in the Δ^2 form (Δ gap between the antibonding symmetric and antisymmetric combinations derived from each magnetically active atomic orbital of the manganese atoms, according to the Hoffmann model),[12] indicate that the superexchange through the N(11)–N(12)–N(11C) bridge occurs mainly through the two d*xz* and d*yz* interactions, whereas the dz^2 pathway contribution is negligible due to its quasi-orthogonal position with respect to the nonbonding π orbitals of the bridge (Figure 3). For the second N(21)–N(22)–N(21A) bridge, the lower bond angle enhances the overlap of the dz^2 orbitals with the π MO of the azido group, but the d*xz* interaction simultaneously decreases (Figure 3). Calculation of the $\Sigma\Delta^2$ affords the 0.104 and 0.102 eV^2 values for each bridge, indicating that the antiferromagnetic contributions for the two different bridges are accidentally similar. The main consequence is that the reported compound is assumed to be a structurally alternating 2-D system due to the two nonequivalent bridges, but magnetically the system may be studied as a homogeneous plane.

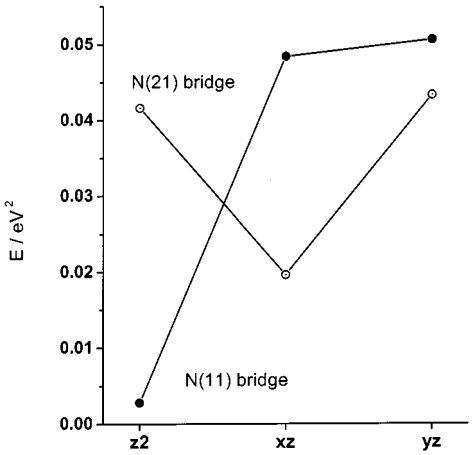

Figure 3. Contribution of each of the three active superexchange pathways for the two different EE bridges of $[Mn(DENA)_2(N_3)_2]_n$

It is remarkable that EE bridges with M–N–N bond angles close to 180° are unusual. To date the only structural and magnetic data for this kind of system was obtained from Mn–N–N–N–Mn units encapsulated in cryptand cavities to force the quasi-linear coordination of the bridge. The magnetic interaction, which was consistent with the theoretical model, was moderately antiferromagnetic.[1]

Magnetic Properties

Susceptibility measurements were performed under a 100 G field in the 300–2 K temperature range. The susceptibility plot shows a maximum placed at 44 K, whereas $\chi_M \cdot T$ decreases continuously on cooling, from 3.87 $cm^3\ K\ mol^{-1}$ at 300 K, and tending to zero at low temperature (Figure 4). This behaviour corresponds to moderate antiferromagnetic coupling and the low temperature shape indicates that canting-like long-range interactions are not effective even at 2 K. Magnetisation measurements at 2 K in the range ±5 T also show behaviour that is normal for an antiferromagnet (Figure 5). Structural data suggest that two *J* superexchange coupling constants are required to fit the susceptibility data, but the above MO calculations show that J_1 is roughly equal to J_2 and so the data were treated as for a homogeneous system. The susceptibility data in the 300–30 K range were fitted with the high-temperature expansion series of Lines[13] for a quadratic-layer Heisenberg antiferromagnet, derived from $H = \Sigma_{nn}(-JS_iS_j)$, where Σ_{nn} runs over all pairs of nearest spins *i* and *j*. The best-fit parameters were $J = -3.42(1)\ cm^{-1}$, $g = 2.01$, $R = 9 \cdot 10^{-5}$. The *J* value and the position of the maximum agree with the value obtained from the simplified expression[13] $kT_{max}/|J| = 1.12\ S\ (S + 1) + 0.10$, from which a $J = -3.1\ cm^{-1}$ value is expected.

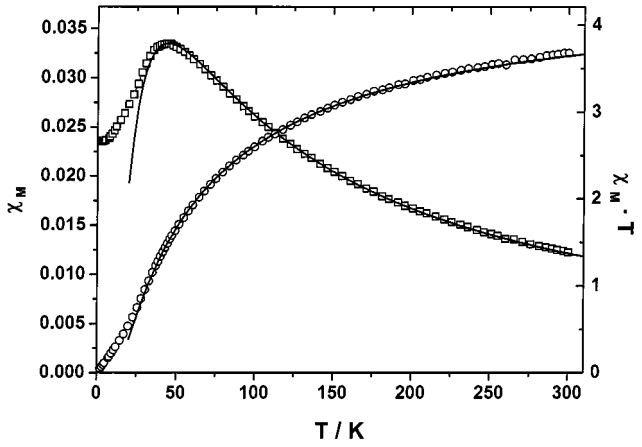

Figure 4. χ_M (dot centered circles) and $\chi_M \cdot T$ (dot centered squares) vs *T* plots for a polycrystalline sample of $[Mn(DENA)_2(N_3)_2]_n$;the solid lines show the best fit under the conditions described in the text

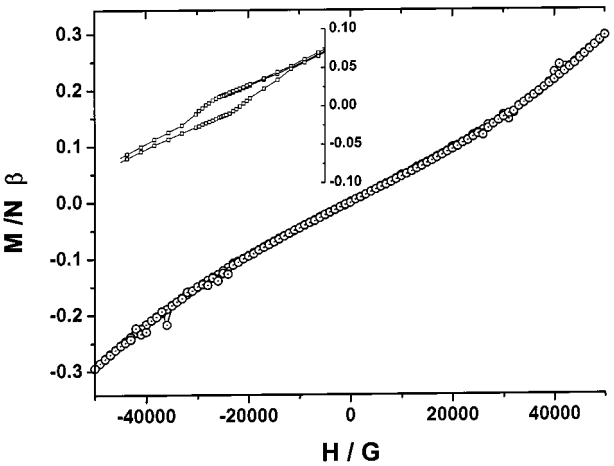

Figure 5. Magnetisation at 2.5 K vs applied field for $[Mn(DENA)_2(N_3)_2]_n$, compared with the related compound $[Mn(Meinc)_2(N_3)_2]_n$ which shows spontaneous magnetisation as a consequence of the structural differences (inset, range ±1.5 T)

This *J* value is comparable with the reported data for the two similar systems with the same topology (Table 1). The main difference between these systems is shown by $[Mn(4\text{-}acpy)_2(N_3)_2]_n$, which shows an ordered phase with a T_C of

28 K, as a consequence of the J value and the angle between the mean Mn equatorial planes, which may induce a canting phenomenon.[4][8a] $[Mn(Me\text{-}i\text{-}nic)_2(N_3)_2]_n$ has a lower J value, which should shift T_C to low temperature. Finally, for the compound reported in this paper, the quasi-parallel main axis of the coordination octahedron of the manganese atoms avoids the canting possibility.

The EPR spectrum consists of a sharp isotropic line centred at $g = 2.00$. Linewidth mainly depends on two factors: superexchange narrowing and dipolar broadening. When structural data, which show Mn···Mn intraplane distances greater than 6.5 Å are included, dipolar effects, if present, should be extremely weak, whereas the relatively high constant coupling of –3.4 cm^{-1} has a strong effect in narrowing the linewidth. The experimental spectrum shows a linewidth of 30 G, similar to the 4-acetylpyridine compounds ($J = -3.8$ cm^{-1}) and lower than the linewidth observed for the methylisonicotinate system ($J = -2.2$ cm^{-1}); this confirms the above assumptions. The dipolar broadening mechanism[14] for a two-dimensional manganese system is an anisotropic property which follows the $a + b\,(1 - \cos^2\theta)^2$ law, i.e., the maximum linewidth appears when the spectrum is measured parallel to the plane and it has the minimum linewidth at the 54.3° magic angle. The possible effects of dipolar broadening were checked in a single-crystal EPR experiment at room temperature, but for all the orientations of the crystal, the spectra were practically identical, showing a minor change in the linewidth between 28–33 G. In recent experiments[3] with the one-dimensional system $[Mn(3,5\text{-lut})_2(\mu_{1,3}\text{-}N_3)_2]_n$ (3,5-lut = 3,5-dimethylpyridine), in which the intrachain Mn···Mn distance is 5.140–5.159 Å, dipolar effects were found (linewidth variation between 40–90 G), but the greater Mn···Mn distance for the DENA compound is experimentally at the upper limit and makes this effect nondetectable.

Experimental Section

General: Infrared spectra (4000–400 cm^{-1}) were recorded in KBr pellets on a Nicolet 520 FTIR spectrophotometer. – Magnetic measurements were carried out with a Quantum Design instrument with a SQUID detector, working in the temperature range 300–2 K. The magnetic field was 100 G for the study of the low-temperature phenomena. Magnetisation measurements were recorded in the ±5 T range of external magnetic field. Diamagnetic corrections were estimated from Pascal Tables. – EPR spectra were recorded at X-band frequency with a Bruker ES200 spectrometer equipped with an Oxford liquid-helium cryostat for variable temperature work.

Synthesis of the Compound: The title complex $[Mn(DENA)_2(N_3)_2]_n$ (**1**) was synthesised by the dropwise addition of 5 mL of an aqueous solution of NaN_3 (0.42 g, 6.5 mmol) to an ethanolic solution mixture, about 30 mL, of manganese chloride trihydrate (0.59 g, 3 mmol) and 1.43 g (8 mmol) of *N*,*N*-diethylnicotinamide. The final clear solution was kept in a refrigerator for several weeks to produce well-formed crystals of the complex. Yield: 0.94 g (ca. 63%). – $C_{20}H_{28}MnN_{10}O_2$ (495.46): calcd. C, 48.4; H 5.7, Mn 11.1, N 28.3, O 6.5; found: C 48.3, H 5.6, Mn 11.2, N 28.5, O 6.4.

IR Spectra: The IR spectrum of the title complex $[Mn(DENA)_2(N_3)_2]_n$ shows bands attributable to the *N*,*N*-diethylnicotinamide ligand at normal frequencies [ν(C=O) at 1627 cm^{-1} (vs)]. In the 2000–2100 cm^{-1} region the complex shows a very strong and broad band, assigned to the asymmetric stretching azide group vibrations [$\nu_{as}(N_3)$] centred at 2092 cm^{-1} (vs). This band appears at normal frequencies; it was compared with that of the linear Mn–N_3–Mn cryptand system previously reported, (2200 cm^{-1}). In the region 1280–1360 cm^{-1} two bands could be attributed to the [$\nu_s(N_3)$] mode: 1378 cm^{-1} (ms) and 1336 cm^{-1} (m). In the far infrared region, two bands attributable to the ν(Mn–N_3) mode around 386 and 374 cm^{-1} and two bands due to the ν[Mn–N(L)] mode around 256 and 236 cm^{-1} were observed.

Crystal Structure Determination and Refinement of the Structure: Single-crystal X-ray data for $[Mn(DENA)_2(N_3)_2]_n$ were collected

Table 2. Crystal data and structure refinement for $[Mn(DENA)_2(N_3)_2]_n$ (**1**)

Empirical formula	$C_{20}H_{28}MnN_{10}O_2$
Formula mass	495.46
Crystal system	monoclinic
Space group	*P*2/*c* (no. 13)
a [Å]	14.153(5)
b [Å]	6.695(3)
c [Å]	13.066(5)
α [°]	90.00
β [°]	101.29(3)
γ [°]	90.00
V [Å^3]	1214.1(8)
Z	2
T [°C]	25(2)
λ(Mo-K_α) [Å]	0.71069
d_{calc} [g cm^{-3}]	1.355
μ(Mo-K_α) [mm^{-1}]	0.581
Max. transmission	1.000
Min. transmission	0.555
Max. peak in final diff. synthesis [eÅ^{-3}]	0.667
Min. peak in final diff. synthesis [eÅ^{-3}]	–0.244
R[a]	0.0492
$R^2\omega\cong$[b]	0.1349

[a] $R(F_o) = \Sigma||F_o| - |F_c||/\Sigma|F_o|$. – [b] $R\omega(F_o)^2 = (\Sigma\{\omega[(F_o)^2 - (F_c)^2]^2\}/\Sigma\{\omega[(F_o)^2]^2\})^{1/2}$.

Table 3. Selected bond lengths [A] and angles [°] for **1**

Mn(1)–N(11)	2.210(3)
(1)–N(21)	2.225(3)
Mn(1)–N(1)	2.291(3)
N(11)–N(12)	1.145(3)
N(21)–N(22)	1.159(3)
C(6)–O(1)	1.236(3)
C(6)–N(2)	1.347(4)
N(1)–Mn(1)–N(1B)	180.0
N(11)–Mn(1)–N(11B)	180.0
N(21B)–Mn(1)–N(21)	180.0
N(1)–Mn(1)–N(11)	90.75(9)
N(1)–Mn(1)–N(11B)	89.25(9)
N(1)–Mn(1)–N(21)	91.2(1)
N(1)–Mn(1)–N(21B)	88.8(1)
N(11)–Mn(1)–N(21)	93.3(1)
N(11)–Mn(1)–N(21B)	86.7(1)
N(11B)–Mn(1)–N(21B)	93.3(1)
Mn(1)–N(11)–N(12)	171.7(2)
Mn(1)–N(21)–N(22)	148.3(2)
N(11)–N(12)–N(11C)	180.0
N(21)–N(22)–N(21A)	178.9(4)

with a modified STOE four-circle diffractometer. Crystal size: 0.50 × 0.34 × 0.24 mm. The crystallographic data, conditions maintained for the intensity data collection and some features of the structure refinement are listed in Table 2. Graphite-monochromated Mo-*Kα* radiation (λ = 0.71069 Å) was used to collect the data set; the ω-scan technique was employed. The accurate unit-cell parameters were determined from automatic centering of 34 reflections (8.5° < θ < 12.9°) and were refined by least-squares methods. 3318 reflections (2531 independent reflections, R_{int} = 0.0370) were collected in the range 2.94° < θ < 26.50°. An intensity decay of 6% for control reflections (–1 –2 0; 0 –2 1; 5 0 2), measured after every set of 100 reflections, was observed during data collection. Corrections were applied for Lorentz-polarization effects, for intensity decay, as well as for absorption, using the DIFABS[15] computer program. The structure was solved by direct methods with the SHELXS-86[16] computer program, and was refined by full-matrix least-squares methods on F^2 with the SHELXL-93[17] program as incorporated in the SHELXTL/PC V 5.03[18] program library, and the graphics program PLUTON.[19] All non-hydrogen atoms were refined anisotropically. The hydrogen atoms were fixed geometrically with the HFIX utility[18] (i.e., hydrogen atoms riding with idealized geometrical values on their parent carbon atoms with fixed distances: CH = 0.93 Å, CH_2 = 0.97 Å and CH_3 = 0.96 Å). Selected bond parameters are given in Table 3.

Atomic positional and thermal parameters, lists of bond lengths and angles, and F_o/F_c values are available as supplementary material from one of the authors (F. A. M.). Crystallographic data (excluding structure factors) for the structure reported in this paper have been deposited with the Cambridge Crystallographic Data Centre as supplementary publication No. CCDC-127494. Copies of the data can be obtained free of charge on application to CCDC, 12 Union Road, Cambridge CB2 1EZ, U. K. [Fax: (int.) +44–1223/336 033; E-mail: deposit@ccdc.cam.ac.uk].

Molecular orbital calculations and magnetic susceptibility properties were explored for the new two-dimensional system *trans*-$[Mn(DENA)_2(N_3)_2]_n$ (DENA = diethylnicotinamide). The compound shows an unusual alternating of the azide bridges with Mn–N–N bond angles of 171.7(2)° and 148.4(2)°. The antiferromagnetic interaction has been correlated with the structural data.

Acknowledgments

This research was partially supported by the CICYT (Grant PB96/0163) and OENB (Grant 6630). F. A. Mautner and M. A. M. Abu-Youssef thank Prof. C. Kratky and Dr. Belaj (University of Graz) for the use of experimental equipment.

[1] A. Escuer, C. J. Harding, Y. Dussart, J. Nelson, V. McKee, R. Vicente, *J. Chem. Soc., Dalton Trans.* **1999**, 223.
[2] A. Escuer, R. Vicente, M. A. S. Goher, F. A. Mautner, *Inorg. Chem.* **1998**, *37*, 782.
[3] M. A. M. Abu-Youssef, A. Escuer, D. Gatteschi, M. A. S. Goher, F. A. Mautner, R. Vicente, *Inorg. Chem.* **1999**, *38*, 5716.
[4] A. Escuer, R. Vicente, M. A. S. Goher, F. A. Mautner, *Inorg. Chem.* **1995**, *34*, 5707.
[5] A. Escuer, R. Vicente, M. A. S. Goher, F. A. Mautner, *J. Chem. Soc., Dalton Trans.* **1997**, 4431.
[6] [6a] M. A. S. Goher, F. A. Mautner, *Croat. Chem. Acta* **1990**, *63*, 559. – [6b] A. Escuer, R. Vicente, M. A. S. Goher, F. A. Mautner, *Inorg. Chem.* **1996,** *35*, 6386**.**
[7] F. A. Mautner, R. Cortés, L. Lezama, T. Rojo, *Angew. Chem. Int. Edit. Engl.* **1996**, *35*, 78.
[8] [8a] A. Escuer, R. Vicente, F. A. Mautner, M. A. S. Goher, *Inorg. Chem.* **1997**, *36*, 3440. – [8b] M. A. S. Goher, N. A. Al-Salem, F. A. Mautner, *J. Coord. Chem.* **1998**, *44*, 119.
[9] H. Y. Shen, D. Z. Liao, Z. H. Jiang, S. P. Yan, B. W. Sun, G. L. Wang, X. K. Yao, H. G. Wang, *Chem. Lett.* **1998**, 469.
[10] [10a] G. De Munno, M. Julve, G. Viau, F. Lloret, J. Faus, D. Viterbo, *Angew. Chem. Int. Ed. Engl.* **1996**, *35*, 1807. – [10b] R. Cortés, L. Lezama, J. L. Pizarro, M. I. Arriortua, T. Rojo, *Angew. Chem. Int. Ed. Engl.* **1996**, *35*, 1810. – [10c] J. Curely, F. Lloret, M. Julve, *Phys. Rev. B* **1998**, *58*, 11465.
[11] C. Mealli, D. M. Proserpio, CACAO program (Computed Aided Composition of Atomic Orbitals), *J. Chem. Educ.* **1990**, *67*, 399.
[12] P. J. Hay, J. C. Thibeault and R. Hoffmann, *J. Am. Chem. Soc.* **1975**, *97*, 4884.
[13] M. E. Lines, *J. Phys. Chem. Solids* **1970**, *31*, 101.
[14] A. Bencini, D. Gatteschi, *EPR of Exchange Coupled Systems*, Springer-Verlag, Berlin Heidelberg **1990**, Chap. 10 and references therein.
[15] N. Walker, D. Stuart, *Acta Crystallogr.* **1983**, *A39*, 158.
[16] G.M. Sheldrick, *SHELXS-86*, Program for the Solution of Crystal Structure. University of Gottingen, Germany, **1986**.
[17] G.M. Sheldrick, *SHELXL-93*, Program for the Refinement of Crystal Structure. University of Gottingen, Germany, **1993**.
[18] *SHELXTL 5.03* (PC-Version), Program library for the Solution and Molecular Graphics. Siemens Analytical Instruments Division, Madison, WI, **1995**.
[19] A. L. Spek, *PLUTON-92*, University of Utrecht, 3584, CH Utrecht, The Netherlands **1992**.

Received June 24, 1999
[I99230]